Journal of Alloys and Compounds 496 (2010) 313–316

Contents lists available at ScienceDirect

Journal of Alloys and Compounds

journal homepage: www.elsevier.com/locate/jallcom

Thermal stability of the $Al_{70}Ni_{10}Ti_{10}Zr_5Ta_5$ amorphous alloy powder fabricated by mechanical alloying

Xiu Wei [a], Xinfu Wang [a], Fusheng Han [a,*], Haowen Xie [b], Cui'e Wen [b]

[a] Key Laboratory of Materials Physics, Institute of Solid State Physics, Chinese Academy of Sciences, Hefei, Anhui 230031, China
[b] Center for Material and Fiber Innovation, Institute for Technology and Research Innovation, Deakin University, Pigdons Road, Geelong, Victoria 3217, Australia

ARTICLE INFO

Article history:
Received 26 September 2009
Received in revised form 29 January 2010
Accepted 4 February 2010
Available online 11 February 2010

Keywords:
Amorphous alloys
Mechanical alloying
Thermal stability

ABSTRACT

An $Al_{70}Ni_{10}Ti_{10}Zr_5Ta_5$ amorphous alloy powder was fabricated by mechanical alloying. The phase structure and characteristic temperatures of the alloy were determined by X-ray diffraction, transmission electron microscopy and differential scanning calorimetry. The glass transition behavior and crystallization kinetics were analyzed using Lasocka and Kissinger functions. The results show that the alloy has a higher crystallization temperature, a higher effective activation energy of crystallization and a wider supercooled liquid region than the previously reported values, suggesting a high thermal stability and promising applications.

1. Introduction

Al-based amorphous alloys have attracted more and more attention in recent years due to their high tensile strength (>1500 MPa) and high bending ductility (180°) [1,2]. Al-based amorphous alloys are among the most prospective light-weight structural materials because their strengths are two to three times higher than those of conventional crystalline aluminum alloys in addition to their very low specific weight [1,3]. The predominant Al-based amorphous alloys include Al–TM (TM: transition metals) system, such as Al–Ni–Ti and Al–Zr–Ni, as well as Al–Zr–LEM (LEM = Fe, Co, Ni and Cu) system [2,4,5]. Since these alloys are usually produced by rapid cooling from liquid state, only limited alloy systems and very small material dimensions can be obtained because of their limited glass forming ability [2–6]. Moreover, these alloys usually show relatively low thermal stability and a narrow supercooled liquid region, limiting their usage in engineering fields. Recently, efforts have been made to improve the thermal stability of Al–TM amorphous alloys by adding rare earth elements or metalloid elements [7–9]. However, the improvement has been insignificant and the attainable supercooled liquid region is still smaller than 50 K.

As is known, mechanical alloying (MA) is an alternative to rapid cooling for fabricating amorphous alloys. Since it is a solid state alloying process, a high cooling rate is not necessary and the alloy composition can be more flexible [10]. Based on the mechanically alloyed amorphous powders, the bulk amorphous component can be fabricated through the powder metallurgy route without strict limitations on product size and shape. It has been reported that many types of amorphous alloy powders can be consolidated into bulk forms via hot pressing [11], spark plasma sintering [12], extrusion [13], high pressure torsion [14] and equal channel angular extrusion [15]. However, since all these consolidation processes are performed at temperatures within the supercooled liquid region, a higher crystallization temperature and a wider supercooled liquid region or higher thermal stability are essential for the consolidation operation [16–20]. Accordingly, studies have been carried out recently to find suitable Al-based amorphous alloy powders for processing corresponding bulk amorphous alloys in our group. An Al-based amorphous alloy powder was fabricated with the composition of (at.%) $Al_{70}Ni_{10}Ti_{10}Zr_5Ta_5$ by mechanical alloying according to the fact that Zr and Ta can improve the thermal stability of Al–Ni–Ti amorphous alloy without impairing its glass forming ability [21,22]. The aim of the present study is to characterize the microstructure and glass transformation features as well as the thermal stability of the amorphous alloy powder to give a basis for the preparation of the corresponding bulk material.

2. Experimental

Elemental Al, Ni, Ti, Zr and Ta powders with a purity of 99.9% and a mean diameter of 70 μm were used as the starting materials. The MA was conducted in a Retsch mill (PM400) using stainless steel cans and bearing steel balls (GCr15) with a ball/powder weight ratio of 20:1 and a rate of 150 rpm. The milling process was paused every 20 h to take a small amount of powder out of the cans for analysis. All the powder operations were performed in a glove box filled with high purity argon gas to avoid contamination. Microstructures of the resultant powders were analyzed

* Corresponding author. Tel.: +86 551 5591435; fax: +86 551 5591434.
E-mail address: fshan@issp.ac.cn (F. Han).

0925-8388/$ – see front matter © 2010 Elsevier B.V. All rights reserved.
doi:10.1016/j.jallcom.2010.02.003

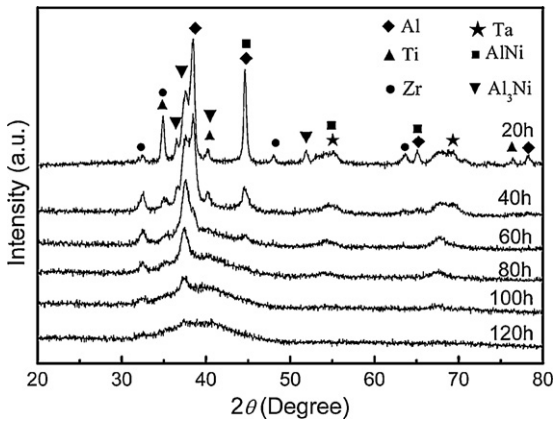

Fig. 1. XRD patterns of mechanically alloyed $Al_{70}Ni_{10}Ti_{10}Zr_5Ta_5$ powders milled for different times.

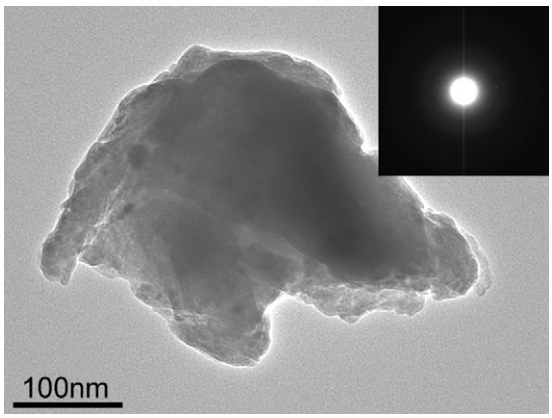

Fig. 2. TEM bright-field image and diffraction pattern of selected area in the $Al_{70}Ni_{10}Ti_{10}Zr_5Ta_5$ powder milled for 120 h.

by X-ray diffraction (XRD, X' Pert Pro MPD) using Cu Kα radiation and transmission electron microscopy (TEM, JEOL 2010) operated at 200 kV with a bright-field image and a selected area diffraction pattern. The samples for TEM examination were put into a pure ethanol solution first, then treated by supersonic apparatus for 10 min and finally dropped onto a copper mesh coated with carbon film. The glass transition temperature (T_g) and crystallization temperature (T_x) were measured by differential scanning calorimetry (DSC, Pyris Diamond) at varied heating rates in a nitrogen atmosphere, in which the T_g was defined as the half-step temperature when the heat flow is equal to the mid-value between the extrapolated heat capacity of liquid and that of a glassy state [23,24].

3. Results and discussion

The XRD patterns of $Al_{70}Ni_{10}Ti_{10}Zr_5Ta_5$ powders milled for different times are shown in Fig. 1. As the powder milled for 20 h, there were several sharp peaks corresponding to pure elements such as Al, Ti, Ta and Zr, and other peaks related to such intermetallic phases as AlNi and Al_3Ni. These peaks gradually became lower and broader and some peaks even disappeared as the milling time increased. According to the Scherrer equation [25], the average size of the crystallite was in the range of 10–50 nm after milling for 20 h. With further increasing the milling time, for example 80 h, a broad halo peak appeared in the range of diffraction angle, 2θ, from 30° to 50°, which indicates the formation of an amorphous phase. After milling for 120 h, all the diffraction peaks typical of crystalline phases disappeared, indicating the completion of the vitrification process. The structure of powders can be developed in such a way that Ni dissolved into Al to form Al–Ni solid solution and some intermetallic phases at the early milling stage, after which the Ta dissolved into Al–Ni solid solution followed by the dissolution of Ti and Zr into Al–Ni–Ta solid solution [10,26].

In terms of thermodynamic fundamentals, a small Gibbs free energy ΔG is necessary for the glass formation of a system. From the Gibbs equation $\Delta G = \Delta H - T\Delta S$, where ΔH is the enthalpy of fusion; T is the absolute temperature and ΔS is the entropy of fusion, it is obvious that ΔG changes in the opposite direction to ΔS, and a low ΔG means a small enthalpy of fusion ΔH and a large entropy of fusion ΔS. For a multiple component system, the larger the difference between atomic sizes, the smaller the Gibbs free energy, because the former will increase the packing density of atoms in the supercooled liquid, giving rise to increased liquid/solid interfacial energy or decreased ΔH. During the MA, the grain size will gradually decrease while the lattice strain and distortion will increase with the increase of the milling time, leading to an increase in the structure defects and a decrease in the free energy of the crystalline phase. The vitrification occurs once the free energy of the constituent phase is below that of the crystalline phase. According to the atomic sizes (nm) of the present alloy, that is Al 0.143, Ni 0.125, Ta 0.143, Zr 0.162 and Ti 0.147, the above dissolution process, which was caused by the difference in atomic sizes between components, accelerates the formation of the amorphous structure [27]. The composition of the present alloy is closed to that predicted by the dense cluster-packing model of Al–Zr–Ti–Ni–Ta system [28,29], i.e. $Al_{68}Zr_8(Ti,Ta)_8Ni_{16}$.

Fig. 2 shows the TEM bright-field image with selected area diffraction pattern of the 120 h milled powder. It can be seen that the particles show a very fine and homogeneous microstructure, and there is a diffusive halo typical of an amorphous phase, being in agreement with the XRD results shown in Fig. 1. It should be noticed that the image shown in Fig. 2 has different black–white contrasts, which can be attributed to clustered particles with different thicknesses that are very difficult to divide by ultrasonic treatment.

To investigate the glass transition and crystallization behavior in more detail, DSC measurements were carried out at varied heating rates for the 120 h milled powder. As can be seen in Fig. 3(a) and Table 1, the powder exhibited the endothermic characteristic of glass transitions and an exothermic crystallization peak. As the heating rate increased, the glass transition temperature (T_g), the onset crystallization temperature (T_x^{onset}) and the crystallization temperature peak (T_x^{peak}) increased, while the supercooled liquid region $\Delta T_x = T_x^{onset} - T_g$ decreased. Obviously, the elevation of T_g is larger than that of T_x^{onset}. As is known, glass transition and crystallization temperatures have the following relationship or Lasocka's relationship with heating rate β [30]:

$$T_p = A + B \ln \beta \quad (1)$$

where A and B are the constants relating to the material itself and which can be determined jointly by DSC measurements and Eq. (1); T_p is the glass transition temperature or crystallization temperature. For the present alloy, the following relationships of T_p with $\ln \beta$ can be obtained:

$$T_g = 640.9 + 25.1 \ln \beta \quad (2)$$

$$T_x^{onset} = 753.2 + 18.4 \ln \beta \quad (3)$$

Table 1
The glass transition temperature (T_g), Crystallization temperatures T_x^{onset} and T_x^{peak} of the $Al_{70}Ni_{10}Ti_{10}Zr_5Ta_5$ alloy powder after milled for 120 h at different heating rates.

	β (K/min)				
	10	20	30	40	50
T_g (K)	701	715	722	732	744
T_x^{onset} (K)	797	806	814	822	826
T_x^{peak} (K)	813	824	830	837	842

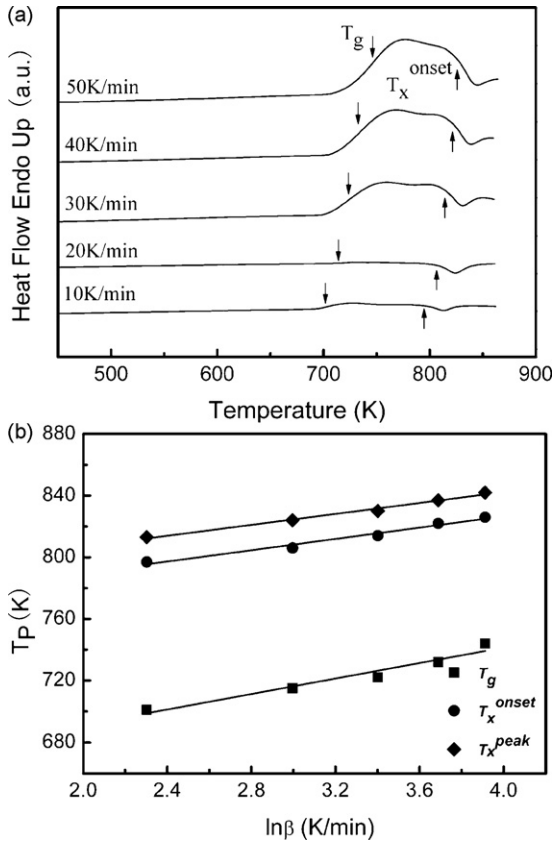

Fig. 3. (a) DSC curves of the $Al_{70}Ni_{10}Ti_{10}Zr_5Ta_5$ powder milled for 120 h and (b) Lasocka plots showing the dependence of characteristic temperatures on heating rates of $Al_{70}Ni_{10}Ti_{10}Zr_5Ta_5$ powder milled for 120 h.

$$T_x^{peak} = 771.3 + 17.8\ \ln\ \beta \tag{4}$$

From these equations and Fig. 3(b), it can easily be seen that the characteristic temperatures follow a linear relationship with $\ln\beta$, in which T_g has the strongest dependence on the heating rate. This is why T_g increases more quickly than T_x^{onset}. This phenomenon has also been observed in a Zr-based metallic glass [31].

It can be observed that both the T_x^{onset} and ΔT_x of the 120 h milled powder are greater than previously reported values for other Al-based amorphous alloys [2,6,9,18,32], suggesting that it is more stable than those of previously reported Al-based amorphous alloys [33]. The comparison of the crystallization temperatures T_x^{onset} and the supercooled liquid region ΔT_x between the $Al_{70}Ni_{10}Ti_{10}Zr_5Ta_5$ alloy powder and relevant alloys are shown in Table 2. It has been known that adding early transition metals (in the IV–VI group) into Al–Ni–Ti or Al–Ni–Zr ternary alloys can promote the interactions among the constituent elements of the alloy and thus enhance the glass forming ability [1,6]. In addition, if the added early transition metals have relatively high melting points they can also improve the thermal stability and increase the characteristic temperatures of amorphous alloys [6,21,22,34]. Therefore, the improvement of the thermal stability of the present alloy should be mainly attributed to the effect of Ta.

Table 2
Crystallization temperatures T_x^{onset} and the supercooled liquid region ΔT_x of the $Al_{70}Ni_{10}Ti_{10}Zr_5Ta_5$ alloy powder compared with that of relevant alloys.

Alloys system	T_x^{onset} (K)	ΔT_x	Reference
$Al_{85}Y_8Ni_5Co_2$	573	29	[9]
$Al_{85}Y_6Ni_5Co_2Zr_2$	597	47	[9]
$Al_{85}Y_6Ni_5Co_2Sc_2$	612	51	[9]
$Al_{85}Ni_{10}Ce_5$	543	16	[31]
$Al_{80}Ni_{10}Ti_{10}$	500	–	[25]
$Al_{75}Ni_{10}Ti_{10}Zr_5Ta_5$	814	92	Present study

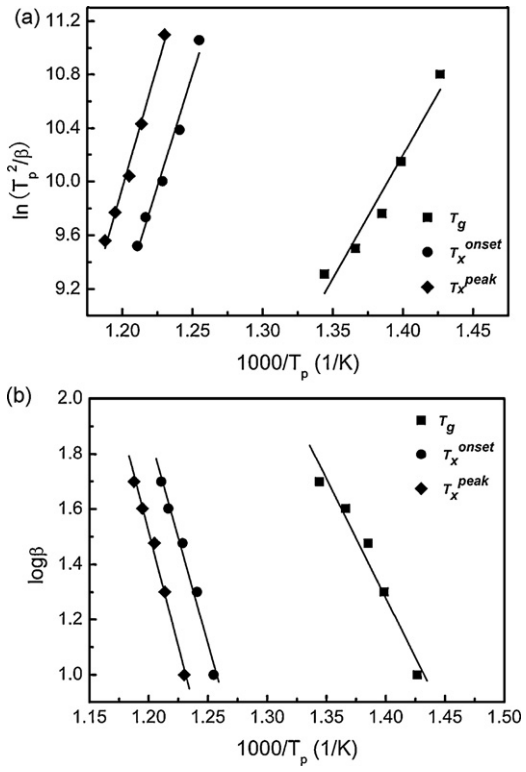

Fig. 4. Kissinger plots (a) and Ozawa plots (b) of T_g, T_x^{onset} and T_x^{peak} of the amorphous $Al_{70}Ni_{10}Ti_{10}Zr_5Ta_5$ powder.

The activation energy of the glass transition and the crystallization of the present amorphous alloy can be estimated by the following Kissinger equation [35]:

$$\ln\left(\frac{T_p^2}{\beta}\right) = \frac{E}{R_g T_p} + c_1 \tag{5}$$

where R_g is the gas constant, c_1 is a constant and E is the activation energy. Based on the results in Fig. 3(a), the following relationships of $\ln(T_p^2/\beta)$ with $1/T_p$ can be obtained:

$$\ln\left(\frac{T_g^2}{\beta}\right) = -15.6 + \frac{18404}{T_g} \tag{6}$$

$$\ln\left(\frac{(T_x^{onset})^2}{\beta}\right) = -31.1 + \frac{33536}{T_x^{onset}} \tag{7}$$

$$\ln\left(\frac{(T_x^{peak})^2}{\beta}\right) = -33.9 + \frac{36523}{T_x^{peak}} \tag{8}$$

By plotting $\ln(T_p^2/\beta)$ against $1000/T_p$ using the data in Fig. 3(a), as shown in Fig. 4(a), the related effective activation energies obtained are 1.59 ± 0.2 eV for T_g, 2.90 ± 0.24 eV for T_x^{onset} and 3.15 ± 0.18 eV for T_x^{peak}.

On the other hand, the dependence of the characteristic temperatures on the heating rate can also be described by the Ozawa equation [36]:

$$\log\ \beta = -0.4567\left(\frac{E}{R_g T_p}\right) + c_2 \tag{9}$$

where c_2 is a constant. Similarly, by plotting $\log\beta$ against $1000/T_p$, as shown in Fig. 4(b), the related effective activation energies

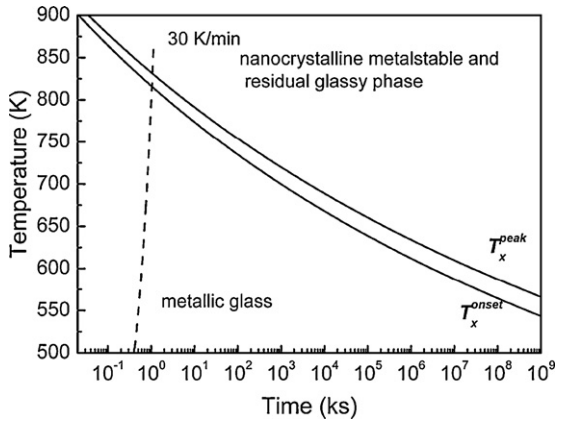

Fig. 5. Continuous heating transformation diagram of the $Al_{70}Ni_{10}Ti_{10}Zr_5Ta_5$ amorphous alloy, in which the dashed line represents a heating rate of 30 K/min.

obtained are as follows: 1.62 ± 0.19 eV for T_g, 2.88 ± 0.23 eV for T_x^{onset} and 3.13 ± 0.17 eV for T_x^{peak}, which are very closed to those obtained by the Kissinger equation.

It should be noticed that the above effective activation energy of crystallization is 3.15 ± 0.18 eV or 303 ± 17.0 kJ/mol, which is higher than that observed in other Al-based amorphous alloys without Ta. For example, it is 167.27 kJ/mol in $Al_{85}Ni_{12.5}Ti_{2.5}$ [2], and 255 kJ/mol in $Al_{88}Ni_6La_6$ [37]. This demonstrates that the thermal stability of an Al-based amorphous alloy can be improved by adding the early transition metal element Ta.

In fact, it is not sufficient to evaluate the thermal stability of amorphous alloys only through the crystallization temperature and the supercooled liquid region width because these are dependent upon the heating rate. Other criteria are also necessary such as the time–temperature–transition diagram built by an isothermal process or a continuous heating transformation diagram (CHT) etc. [38–40]. To get the CHT of the present alloy, Eq. (5) was transformed into the following form:

$$\beta = T_p^2 \exp\left(\frac{E}{R_g T_p} + c_1\right) \tag{10}$$

The heating time (t_h) is given by [38]:

$$t_h = \frac{T_p - 298}{\beta} = \frac{T_p - 298}{T_p^2 \exp(E/R_g T_p + c_1)} \tag{11}$$

By substituting c_1 and E/R_g yielded from Eqs. (7) and (8) into Eq. (11), we get:

$$t_x^{onset} = \frac{T_x - 298}{T_x^2 \exp(-33536/T_x + 31.1)} \tag{12}$$

$$t_x^{peak} = \frac{T_x - 298}{T_p^2 \exp(-36523/T_p + 33.9)} \tag{13}$$

Then by substituting a series of given T_x and T_p values into Eqs. (12) and (13), we get the changes of T_x and T_p with heating time, as shown in Fig. 5, in which the dashed line indicates a situation at the heating rate of 30 K/min. It can be seen from Fig. 5 that the onset and peak crystallization temperatures decrease to 500 K in more than 3.1536×10^9 ks or 100,000 years, suggesting that the present $Al_{70}Ni_{10}Ti_{10}Zr_5Ta_5$ alloy is thermally stable indeed.

4. Conclusions

An $Al_{70}Ni_{10}Ti_{10}Zr_5Ta_5$ amorphous alloy was fabricated by mechanical alloying. The alloy exhibits a high crystallization temperature, a high effective activation energy of crystallization, a wide supercooled liquid region and high thermal stability compared with previously reported Al-based amorphous alloys without Ta. The effective activation energies of crystallization were calculated using both the Kissinger and the Ozawa equations to be about 3.13 and 3.15 eV, respectively.

Acknowledgements

This work is supported by the National Basic Research Program of China (No. 2006CB601201), the National Natural Science Foundation of China (No. 50871107) and Science and Technology Program of Anhui Province, China (No. 07010302211).

References

[1] A. Inoue, Prog. Mater. Sci. 43 (1998) 365–520.
[2] D.H. Kim, W.T. Kim, Mater. Sci. Eng. A 385 (2004) 44–53.
[3] Y. He, S.J. Poon, G.J. Shiflet, Science 241 (1988) 1640–1642.
[4] H. Yang, K.Y. Lim, Y. Li, J. Alloys Compd. 489 (2010) 183–187.
[5] L. Wang, L. Ma, H. Kimura, A. Inoue, Mater. Lett. 52 (2002) 47–52.
[6] A.P. Tsai, A. Inoue, T. Masumoto, Metall. Trans. 19A (1988) 1369–1371.
[7] C. Triveño Rios, S. Suriñach, M.D. Baró, C. Bolfarini, W.J. Botta, C.S. Kiminami, J. Non-Cryst. Solids 354 (2008) 4874–4877.
[8] K.K. Song, X.F. Bian, J. Guo, X.L. Li, M.T. Xie, C.J. Dong, J. Alloys Compd. 465 (2008) L7–L13.
[9] D.V. louzguine-Luzgin, A. Inoue, Appl. Phys. Lett. 88 (2006) 011911.
[10] C. Suryanarayana, Prog. Mater. Sci. 46 (2001) 1–184.
[11] K.G. Prashanth, S. Scudino, B.S. Murty, J. Eckert, J. Alloys Compd. 477 (2009) 171–177.
[12] G. Xie, D. Louzguine-Luzgin, H. Kimura, A. Inoue, Appl. Phys. Lett. 90 (2007) 241902.
[13] K.B. Surreddi, S. Scudino, M. Sakaliyska, K.G. Prashanth, D.J. Sordelet, J. Eckert, J. Alloys Compd. 491 (2010) 137–142.
[14] A.R. Yavari, W.J. Botta Filho, R.Z. Valiev, Scripta Mater. 46 (2002) 711–716.
[15] O.N. Senkov, D.B. Miracle, J.M. Scott, S.V. Senkova, J. Alloys Compd. 365 (2004) 126–133.
[16] Y.Z. Yue, J. Non-Cryst. Solids 354 (2008) 1112–1118.
[17] Y.Z. Yue, J. Non-Cryst. Solids 355 (2009) 737–744.
[18] Z.H. Huang, J.F. Li, Q.L. Rao, Y.H. Zhou, Intermetallics 16 (2008) 727–731.
[19] L.N. Hu, Y.Z. Yue, J. Phys. Chem. C 113 (2008) 15001–15006.
[20] G.H. Li, X.F. Bian, K.K. Song, J. Guo, X.L. Li, C.D. Wang, J. Alloys Compd. 471 (2009) L47–L50.
[21] W. Liu, W.L. Johnson, J. Mater. Res. 11 (1996) 2388–2392.
[22] W.H. Wang, Prog. Mater. Sci. 52 (2007) 540–596.
[23] M.E. Brown, Introduction to Thermal Analysis: Techniques and Applications, Kluwer Academic Publishers, USA, 2004, pp. 55–90.
[24] ASTM, E 1356-98: Standard Test Method for Assignment of the Glass Transition Temperatures by Differential Scanning Calorimetry or Differential Thermal Analysis, American Society for Testing and Materials, 1998.
[25] H.P. Klug, L.E. Alexander, X-ray Diffraction Procedures for Polycrystalline and Amorphous Materials, Wiley, New York, 1954, pp. 491–538.
[26] A. Samanta, I. Manna, P.P. Chattopadhyay, Mater. Sci. Eng. A 464 (2007) 306–314.
[27] A. Takeuchi, A. Inoue, Mater. Trans., JIM 46 (2005) 2817–2829.
[28] D.B. Miracle, Acta Mater. 54 (2006) 4317–4336.
[29] D.B. Miracle, Nat. Mater. 3 (2004) 697–702.
[30] M. Lasocka, Mater. Sci. Eng. 23 (1976) 173–177.
[31] G. He, G.L. Chen, Z. Bian, Intermetallics 8 (2000) 481–485.
[32] H. Yang, T.Q. Wang, Y. Li, J. Non-Cryst. Solids 354 (2008) 3473–3479.
[33] A. Inoue, Mater. Trans., JIM 36 (1995) 866–875.
[34] W.H. Wang, Q. Wei, H.Y. Bai, Appl. Phys. Lett. 71 (1997) 58–60.
[35] H.E. Kissinger, Anal. Chem. 29 (1957) 1702–1706.
[36] T. Ozawa, J. Therm. Anal. 2 (1970) 301–324.
[37] K.L. Sahoo, M. Wollgarten, J. Haug, J. Banhart, Acta Mater. 53 (2005) 3861–3870.
[38] D.V. Louzguine, A. Inoue, Scripta Mater. 47 (2002) 887–891.
[39] D.V. Louzguine, A. Inoue, Appl. Phys. Lett. 81 (2002) 2561–2562.
[40] L. Xia, Y.D. Dong, Mod. Phys. Lett. B 20 (2006) 225–231.